AUTOMATED LATTICE OPTIMIZATION OF HINGE FITTING WITH DISPLACEMENT CONSTRAINT

by

VIGNESH DAKSHNAMOORTHY

Presented to the Faculty of the Graduate School of

The University of Texas at Arlington in Partial Fulfillment

of the Requirements

for the Degree of

Master of Science in Mechanical Engineering

THE UNIVERSITY OF TEXAS AT ARLINGTON

December 2016

Acknowledgements

I would like to express my gratitude to my supervisor, Dr. Robert M Taylor, whose expertise, understanding, support and patience, added considerably to my graduate experience. I would also like to thank my committee members Dr. Ashfaq Adnan and Dr. Kent Lawrence for their valuable time and inputs.

Moreover, I am really grateful for the help offered by Altair Engineering, especially Blaise Cole, Hedison Mui, and Chayan Basak, for their support of this work and my family for their constant support, understanding and care.

Finally, I would like to acknowledge, University of Texas at Arlington and Department of Aerospace and Mechanical Engineering for providing a great opportunity to nurture my interest.

November 10, 2016

Abstract

AUTOMATED LATTICE OPTIMIZATION OF HINGE FITTING WITH DISPLACEMENT CONSTRAINT

Vignesh Dakshnamoorthy, MS

The University of Texas at Arlington, 2016

Supervising Professor: Robert M Taylor

Additive manufacturing enables fabrication of complex lattice cell structures that are not manufacturable using conventional methods. In order to exploit this lattice capability in structural designs, the effect on structural performance must be considered. This paper uses a goose neck door hinge component to illustrate the effects of lattice structure optimization when stiffness criteria drive part design. The effect of intermediate lattice cell density parameters on resulting lattice configurations from automated lattice structure optimization are studied and it is found that the compliance of the model depends upon the range of intermediate density elements present. The paper then compares the effect of a displacement constraint on optimized weight from rib-stiffened and lattice-stiffened shell models. It is shown that optimized weight results from the lattice configuration depend on part stiffness requirements. The results show that lattice structures can be successfully implemented in weight-critical components where relaxation in displacement constraint is acceptable.

Table of Contents

List of Illustrations

List of Tables

Chapter 1

Introduction

Additive manufacturing (AM), also popularly known as 3D Printing is a layer based manufacturing approach in which a complete three-dimensional part is fabricated by adding materials layer by layer [1]. Due to this layer based additive approach, parts with higher geometrical complexity can be fabricated with ease and increase in complexity does not affect the cost of the process as in the case of conventional methods. This capability provides the designer with higher design freedom to optimize the part design towards physics of the problem for optimum performance rather than being limited by manufacturing constraints [2].

One of the capabilities enabled by additive manufacturing is Hierarchical complexity, i.e., the ability to build features at multiple size scales: micro, meso and macro [1]. This paper focuses on the meso scaled repetitive cellular structures like lattice structures. These cellular structures can be designed in such a way that they can be used to fill certain regions of a geometry. From structural aspect, the main advantage provided by lattice structure is high strength to weight ratio when being used to target mass reductions [3]. Also, lattice structures provide good energy absorption, thermal and acoustic characteristics [1]. They can also be used as support structures in several additive processes with minimum support material usage [4].

Lattice structures are inspired from the unique repetitive arrangement of atoms and the bonds between them in crystalline solids. Similarly, in this case, these structures are modelled as interconnected struts between nodes in terms of unit cells and these unit cells

are repeated in three- dimensional space to create a truss like structure [5]. The main parameters that are to be controlled in a unit cell are the end diameters of each lattice member and the cell type. Though, there are several types of unit cells, this paper focuses on the use of cubic hexahedral cells.

Chapter 2

Background

Previous works performed in the field of lattice structures, topology optimization, lattice optimization and the effects of lattice optimization on part stiffness are discussed in this section.

2.1 Lattice Structures

Due to the advancement in AM, there has been a considerable increase in research in the area of cellular structures especially lattice structures. Significant amount of work has been done to investigate the applications and properties of lattice cells. Stuecker et al. [6] has shown that periodic lattice filters can be used efficiently in casting of molten metals as a replacement to ceramic foam filters. Additionally, due to its excellent thermal properties, heat exchangers are modeled after a tetrahedron diamond lattice design by Heidrich et al. [7] and in the field of metal AM, lattice cells are widely used as support structures leading to minimal support material usage (Hussein et al.) [8].

Extensive research has also been done on lattice cell parameters and properties. Most commonly, strut thickness is considered as a key design variable in a lattice unit cell. Whereas, the work by Tang et al. [5] shows that the orientation of lattice cells plays an important role on structural properties. Iyibilgin et al. [9] observed that lattice structures built using fused deposition modeling process has higher strength compared to specimens with same porosity built using the sparse and sparse-double dense styles. Another work by Maskery et al. [10] demonstrates through experimental testing that the mechanical properties of latticed parts is a function of its unit cell size. Coming to cell structures, octet

truss lattice material is a widely studied cell structure. Deshpande et al. [11] have analyzed the mechanical properties of octet unit cell by considering it as struts that are pin jointed at its vertices and have found good agreement in results between analytical predictions and FE calculations. From [11], Deshpande has also illustrated that the strength of cellular foam materials scales as $\bar{\rho}^{1.5}$ whereas for lattice structures, the strength scales as $\bar{\rho}$ where $\bar{\rho}$ is the relative density of the material. For instance, lattices with a $\bar{\rho}$=0.1 are about three times stronger per unit weight than a typical foam From the above relationship, we can say that lattices are relatively stronger per unit weight than foams and this difference is due to the nature of material deformation [1]: the foam is governed by cell wall deformations whereas lattices stretch and compress.

Apart from research works on lattice cellular structures, cell properties and applications, vast amount of works has been performed in the area of lattice failure and its mechanisms. Doyoyo and his team [12] have demonstrated that two strut geometric parameters: strut-level strengthening and slenderness ratio influence the size and shape of the failure surfaces when subjected to multi-axial loads. This also affects the microscopic deformation mechanisms leading to macroscopic failures. A methodology was proposed by Labeas and Sunaric [13] to predict the structural response and the failure process of three different cellular core types under compressive loads. Their numerical results shows that the structural response is highly influenced by geometrical parameters such as strut aspect ratio and unit cell size and shape. They have also shown that plateau stress of all core types increases as the unit cell size decreases. Another work by Shen et al. [14] have shown that [±45°] and [±45°, 90°] lattice structures failed under bending and stretching modes of failure whereas [0°, ±45°] lattice cells failed due to buckling of vertical pillars. Masoumi et al. [15] have presented a numerical method based on asymptotic

homogenization theory for predicting the effect of unit cell shape on the fatigue strength of hexagonal and square lattices. This numerical method demonstrates that the shape of the unit cell has a major influence on the fatigue failure of lattice material under multi-axial cyclic loading.

2.2 Topology Optimization

A problem in topology optimization is formulated such that optimal spatial distribution of material is obtained for a given set of loads and boundary conditions to minimize/maximize certain objective function $f(x)$ [16] while satisfying its design constraints. Any optimization problem can be expressed in a general form [17] as shown in equation (1).

$$\begin{aligned} &\text{Minimize/Maximize} && f(x) \\ &\text{Such that} && h_j(x) = 0 \quad j = 1,2,\dots . n_h \\ & && g_k(x) \leq 0 \quad k = 1,2,\dots . n_k \end{aligned} \tag{1}$$

Where h_j and g_k are constraints, j and k are the number of equality and inequality constraints, respectively. Topology optimization is performed to obtain a concept design which requires further fine tuning by shape and sizing optimizations. Several optimization algorithms are developed for this purpose. Initially in 1988, homogenization method based on square and rectangular holes was introduced by Bendsoe and Kikuchi [18] and it was further developed by Rozvany into “SIMP” and he has performed a detailed evaluation of other available optimization algorithms in his work [19]. The homogenization method introduced by Bendsoe and Kikuchi was modified for shape and topology optimization of

linear elastic structures by Suzuki et al.[20]. Another optimization method was introduced by Xie and Steven [21] in 1993 called the Evolutionary Structural Optimization “ESO”. The basic concept of this method is to remove inefficient material from a structure so that the structure slowly evolves towards optimal topology under certain rejection criteria such as stiffness, frequency, buckling etc. One of the main advantages of ESO method is that it takes a relatively small amount of time for solving a problem and it is simple to program via the FEA packages. The same authors have demonstrated the ESO method for dynamic problems [22] where at the end of each eigen-value analysis, a part of material is removed from the structure so that frequency of the resulting structure is moved towards optimum value. These results agree with the same optimization problem performed by other optimization methods. Later in 2002, a numerical method was presented by Wang et al.[23] Here, the design boundaries are represented by level set models. This optimization method proves effective and flexible in handling topological changes, fidelity of boundary representation and degree of automation. A 99 line MATLAB code was written by Sigmund [24] to perform topology optimization for compliance minimization of statically loaded structures. As a successor to the 99 line code written by Signmund, Andreassen et al [25] has improvised it to 88 line MATLAB code by taking advantage of MATLAB’s loop vectorization, memory pre-allocation and restructuring the old program. The latest version has several improvements like inclusion of density filter and increased optimization speed and efficiency without sacrificing the readability of the code. This paper uses the same example from Sigmund’s [24] work to demonstrate the code’s efficiency. The design region is discretized by square finite elements and a modified SIMP method is chosen for solving the optimization problem. Each element e is assigned a density x_e and its Young’s Modulus E_e is calculated as shown in equation (2).

$$E_e(x_e) = E_{min} + x_e^p(E_0 - E_{min}) \qquad x_e \in [0,1] \qquad (2)$$

Where, E_0 is the stiffness of the material and E_{min} is used for preventing singularity of stiffness matrix. It is a very small stiffness assigned to void regions and p is the penalization factor. Equation (2) corresponds to the modified SIMP method which differs from the classical SIMP method used in the original paper by the usage of E_{min} term. The classical SIMP method avoids the singularity of stiffness matrix by imposing a lower limit slightly larger than 0 for the densities x_e. The mathematical formulation of the problem is given in equation (3) and it is solved by using standard optimality criteria method.

$$\text{Min } x \qquad \mathrm{c(x)} = U^T \mathrm{KU} = \sum_{e=1}^{N} E_e(x_e) u_e^T k_0 u_e$$

$$\text{Such that} \qquad \frac{V(x)}{V_0} = f \qquad (3)$$

$$KU = F$$

$$0 \le x \le 1$$

Where c is the compliance, U and F are the global displacement and force vectors, K is the global stiffness vector, $u_e$is the element displacement vector, $k_0$is the stiffness matrix for an element with unit Young's modulus, x is the element densities, N is the number of elements and $\frac{V(x)}{V_0} = f$ is the volume fraction (design constraint).

OptiStruct performs topology optimization based on density method which is also known as SIMP method and in this method, density of every element is taken as a design

variable in topology optimization process. The density of each element in the final result should have a value of either 0 (void) or 1 (solid). Elements having density value between 0 and 1 are treated as fictitious material and their presence are not meaningful when we are looking for topology of a given material and so they are penalized into voids and solids. OptiStruct provides the user to control over the element discretization using DISCRETE parameter [26]. The penalization technique used here is the “power law representation of elastic properties” [27] as shown in equation (4).

$$\dot{K} = \rho^P K \tag{4}$$

Where $\dot{K}$ and K represents the penalized and real stiffness matrix of the element, ρ represents the density and p is the penalization factor. By default, the penalization factor p takes a value of 1 where no penalty is applied. Whereas on increasing the value of p, influences the tendency of elements in a topology optimization to converge to a material density of either 0 or 1 i.e., higher the penalization value, lower the number of elements that remain between 0 and 1.

2.3 Lattice Optimization

Lattice optimization is an extended step from topology optimization. The main task involved in lattice optimization is to develop an algorithm for designing lattice structures. Several methods have been proposed for designing these cellular structures. For instance, Nguyen et al. [28] proposed a two-step approach for designing conformal lattice structures (CLS) based on an heuristic which assumes, stress distributions are similar in CLS and in a solid body of same shape. As an alternative to the time consuming traditional CAD

software, McMillan et al. [4] have developed a programmatic method for generating lattice structures directly in the STL format and in order to deal with computational and storage complexities in CAD systems caused by large conformal truss structures, a hybrid modeling method was developed by Wang et al. [29]. Further, a size matching and scaling method was developed by Chang et al.[30] for designing meso-scaled lattice structures. Hao et al. [31] have established an image based algorithm for developing periodic lattice structures and have investigated its manufacturability using selective laser melting (SLM) process. A comparison was done between uniform voxel based approach and conformal lattice approach for constructing lattice structures by Park et al.[32]. Finally, another comparative study was done between Particle Swarm Optimization (PSO) and least-squares minimization (LSM) for designing cellular structures by Chu et al. [33]. Later, it was found that PSO was more effective in searching large design spaces whereas LSM converged more quickly than PSO.

This work uses Altair OptiStruct Optimization program [34] for lattice optimization. Some of the limitations of the program include: lattice struts generated are mesh dependent, lattice structures generated can have only circular cross section and inability of cleaning lattice members below a threshold diameter limit.

2.4 Effect of Lattice Optimization on Part Stiffness

This work illustrates the dependence of compliance on lattice structures present in the part. Similarly, Rosen et al. [35] has demonstrated that stiffness of octet-truss structure decreases with increase in number of cells and Cerardi et al. [36] observed the inverse relationship between mechanical properties (stiffness and tensile strength) and the

porosity rate (lattice cells) in three different structures. These results are in agreement with an investigation performed by Sudarmadji et al. [37] who demonstrated the inverse relationship between stiffness and porosity in functionally graded scaffolds using 13 different polyhedral configurations.

Inclusion of lattice structures affect the part's stiffness differently depending upon its element type and the load being applied to it. For instance, figure 1,2 and 3 illustrates a comparison of change in stiffness between a plate (left) and a solid structure (right) upon the addition of lattice structures when subjected to axial and bending loads.

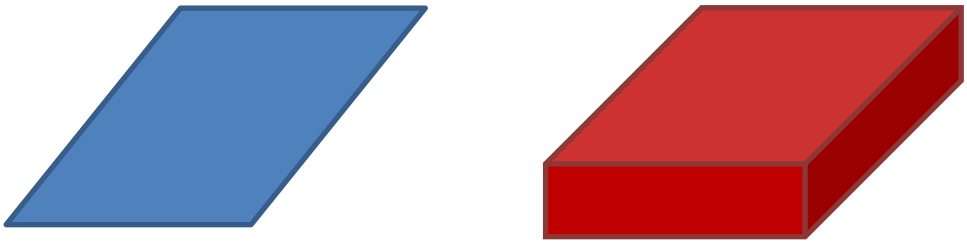

Figure 1: Plate and solid component without lattice structures under axial loads

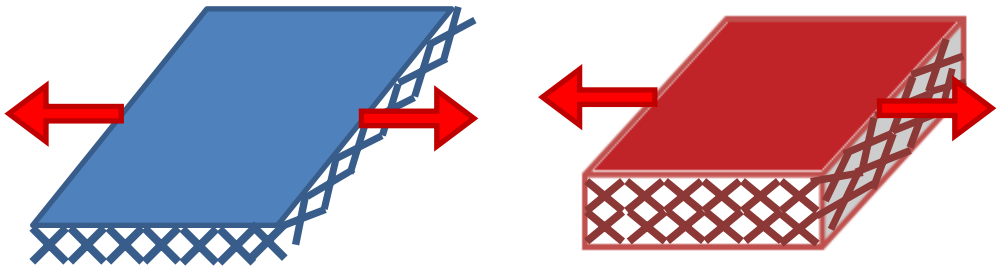

Figure 2: Plate and solid component with lattice structures under axial loads

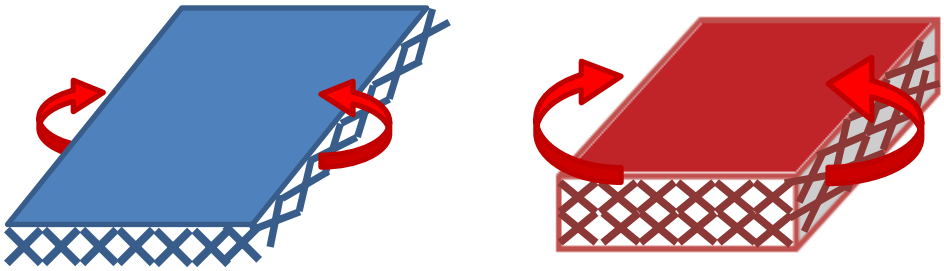

Figure 3: Plate and solid component with lattice structures under bending loads

Under axial loading, lattice structures do not contribute to the stiffness of the plate and its stiffness remains unchanged. Whereas during bending, the structural depth of the plate increases due to the addition of lattice structures which in turn increases its bending stiffness. For a solid component under axial and bending loading conditions, inclusion of lattice structures reduces its mass and stiffness (axial and bending) because solid dense material is replaced by partially dense lattice structures.

Chapter 3

Lattice Structure Design Optimization

This section provides the model details and its topology and lattice optimization results. Further, the effects of intermediate density range and porosity parameter are discussed.

3.1 Hinge Model Details

In this work, a goose neck door hinge is used for illustrating the effects of lattice optimization. This component is used to open doors in aircrafts and automobiles where an abrupt throw out action is necessary to clear an outwardly curved surface or other obstructions [38]. Figure 4 shows a conventional design of the door hinge.

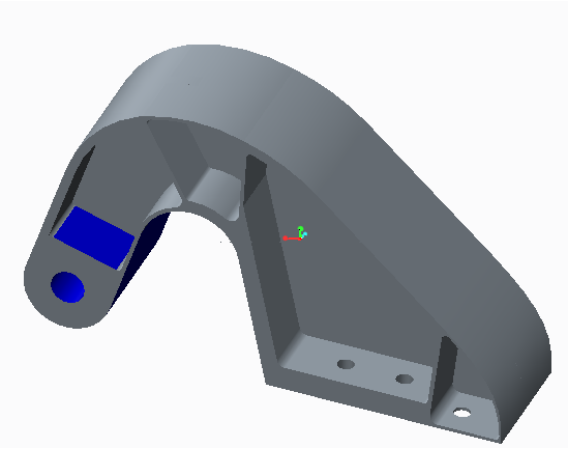

Figure 4: Conventional design of goose neck door hinge

The key area to focus is the location of placement of stiffeners along the hinge neck. The component is assumed to be made up of Aluminum. The blue region is the

design space and the green region called “Lug” is non design space as shown in figure 5. The base of the hinge is constrained by means of six fasteners to the door and lug is the pivoted end. The lug is subjected to four separate loading conditions as shown in the free body diagram [figure 5]. The horizontal load is for opening whereas the vertical load is for closing condition. The other two side loads are to account for inertial forces.

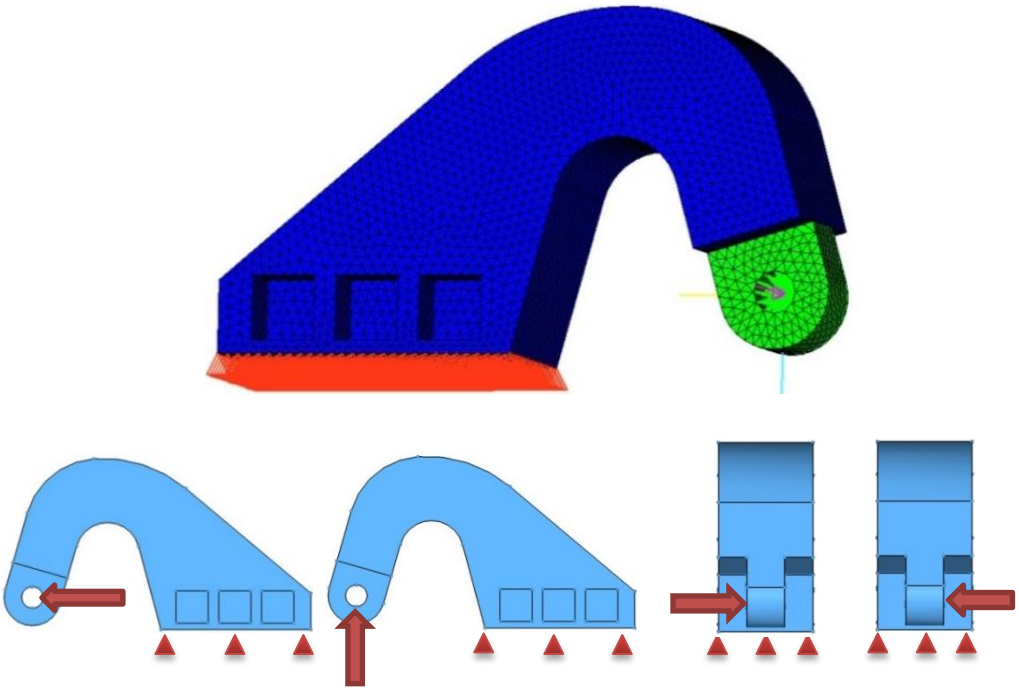

Figure 5: Design Space and Free body diagram of Goose neck door hinge

3.2 Hinge Topology Optimization

This paper is an extension of work done by Taylor et al. [39][40]. Here, Altair’s HyperMesh software is used for preprocessing and OptiStruct solver is used for

optimization. The objective of topology optimization is to obtain the stiffest material distribution for the applied loads and boundary conditions as shown in figure 5 OptiStruct solver is based on DRCO (**D**esign variable, **R**esponse, design **C**onstraint and **O**bjective function) approach.

OptiStruct uses a density based approach to solve topological optimization problems [27]. Under this method, the element density is used as a design variable and it should take a value of 0 (void) or 1 (solid) which makes it a discrete variable leading to higher computational needs. In order to bypass this, element density is treated as a continuous variable between 0 and 1 and any intermediate value represents fictitious material. But the presence of fictitious material are not meaningful in topology solutions. Hence, they are penalized, forcing the final design to be densities of only 0s and 1s. The responses used are volume fraction and weighted compliance. Volume fraction refers to the percent of initial design space to be maintained in the final solution and weighted compliance is the sum of compliance of four individual load cases. Both the responses are global and are defined for the whole structure. A specific percent of volume fraction is used as a constraint and minimizing weighted compliance is the objective function used to obtain the stiffest configuration. Based on the optimization results for various values of volume fraction constraints, 40% is chosen for further analysis as it provides better representation compared to other models.

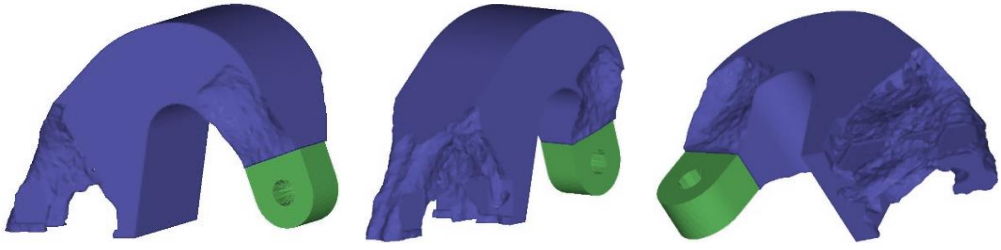

Figure 6: Optimization result for 40% volume fraction constraint

Topology optimization provides an optimum design based on critical load paths which are often not manufacturable through conventional methods. For this purpose, manufacturing constraint such as draw direction is imposed for linear tool access in a particular direction which reduces the optimality of the design to a certain extent but makes it manufacturable [41].

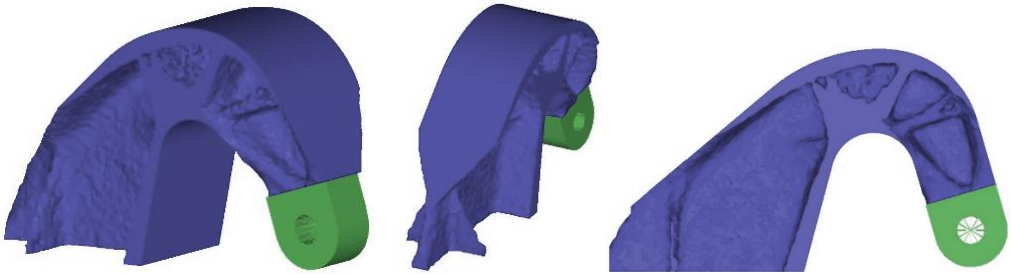

Figure 7: Optimization result – 40% volume fraction with draw direction in Z axis and no holes constraint

The final optimized result as shown in figure 7 resembles I beam section which resists bending during the open and close loading conditions better than other beam cross sections.

Another case study of topology optimization of a similar hinge design was performed. The component is a part of redesign challenge from GrabCAD.com[42]. The objective of this challenge is to redesign a hinge bearing bracket as shown in figure 9 so that its topology and shape are optimized for obtaining highest strength to weight ratio while fitting in the target envelope. This component is optimized using Altair's solidThinking Inspire 2016 version.

The overall design process involves topology optimization of the hinge component under certain optimization constraints, followed by cleaning up of noisy organic result using the PolyNURBS feature from SolidThinking Inspire and fabricating a prototype using fused deposition modelling (FDM) process.

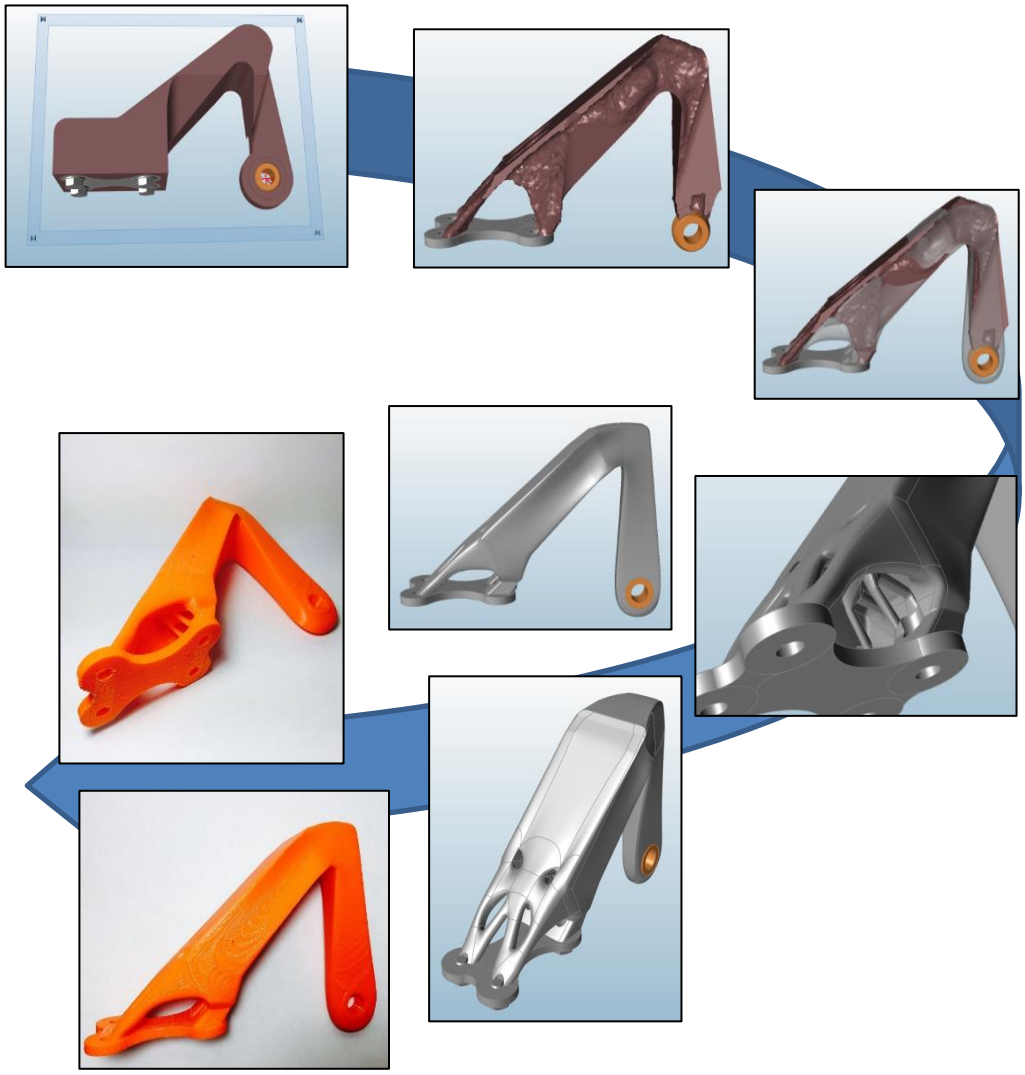

Figure 8: Overall design process

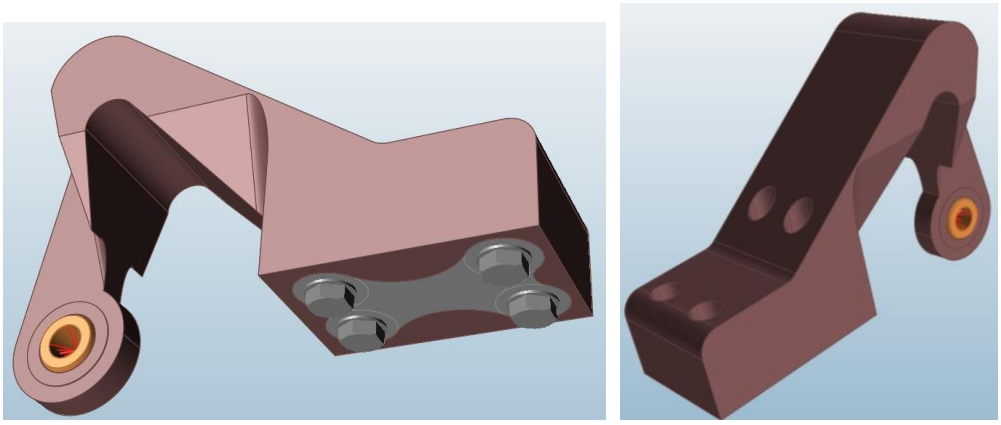

Figure 9: Design space for the bearing bracket

The brown region as shown in the above figure is the design space and the grey region at the bottom with fasteners and the orange bearing region are the non-design regions. The base of the model is constrained using four fasteners and the loads are applied at the center of the non-design bearing region. There are three separate loading conditions as shown in figure 10.

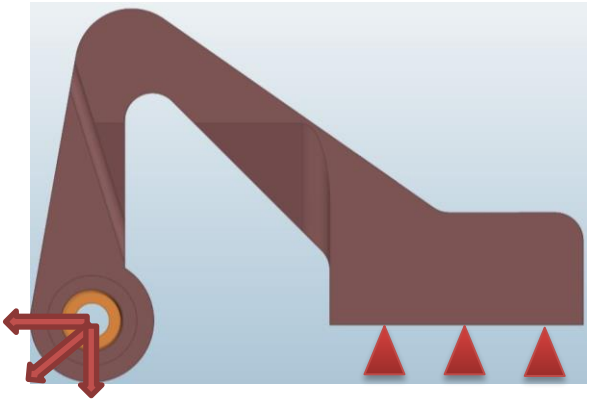

Figure 10: Boundary and loading conditions

Similar to OptiStruct, Inspire uses the DRCO approach for performing topology optimization. The density of elements are taken as design variable and 30% of volume fraction is imposed as design constraint. In order to obtain a stiffest material distribution, maximizing stiffness is applied as an objective function and optimization is performed.

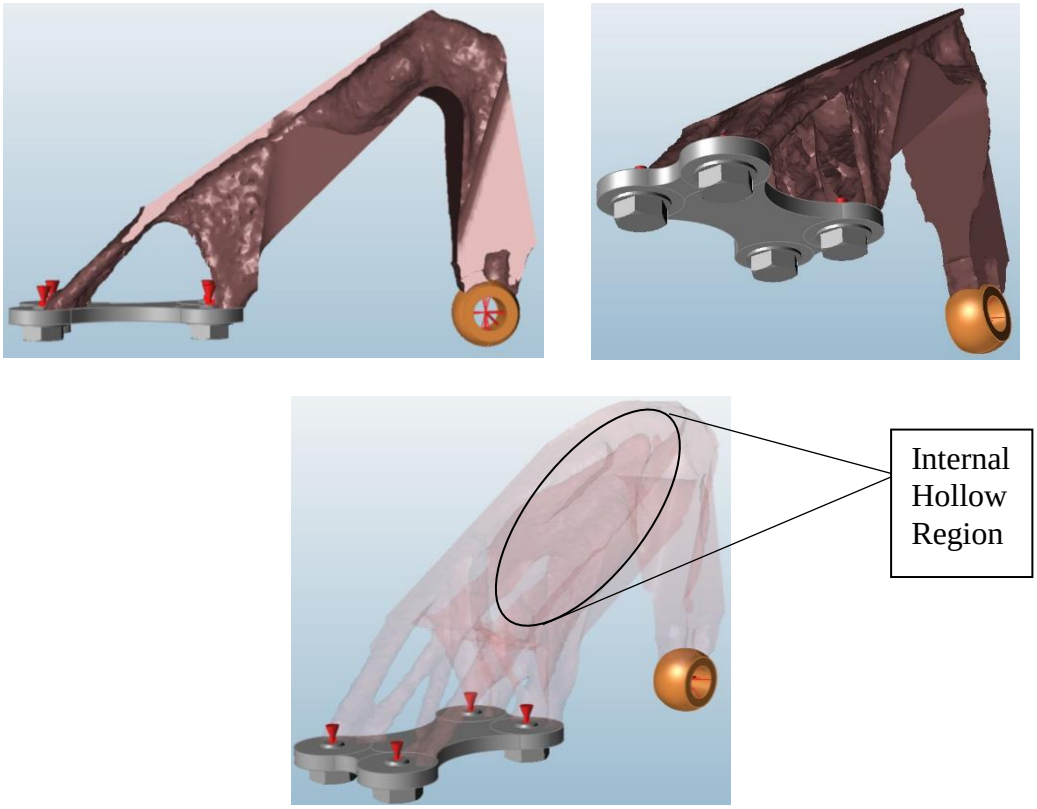

Figure 11: Optimization results for 30% volume fraction constraint

As the manufacturing draw direction constraint is not imposed, the optimization solver provides an organic result with internal hollow regions as shown in figure 11 similar to the OptiStruct solver results in figure 6. The obtained topology optimization result is highly noisy and organic in nature which has to be cleaned prior to further fabrication.

3.2.1 PolyNURBS

Generally in a design cycle, topology optimization for a component is performed initially to obtain optimal shape within a given package space under certain set of loads. The optimization solver uses simulation technology to determine the optimal shape to withstand the applied forces with minimal mass and stress [43] which provides an organic result as seen in figure 6 and figure 11. These results often requires modification/finishing actions to be performed on its geometry by importing into a CAD package before taking it for manufacturing or other processes further downstream.

Inspire 2016 provides one such feature called PolyNURBS with which manufacturable designs can be created easily from organic topology optimization results[44]. This feature allows the user to create solid geometry over the optimized results to create smoother and water tight Non-uniform rational Basis splines (NURBS) [45] which can be further imported into CAD packages for adding final details or directly used for manufacturing.

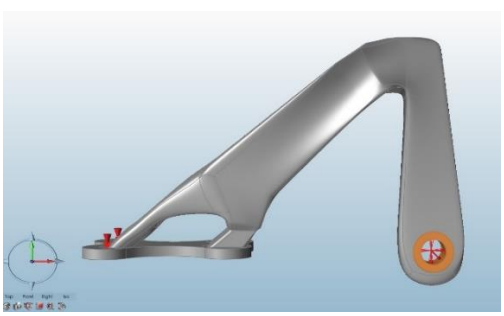

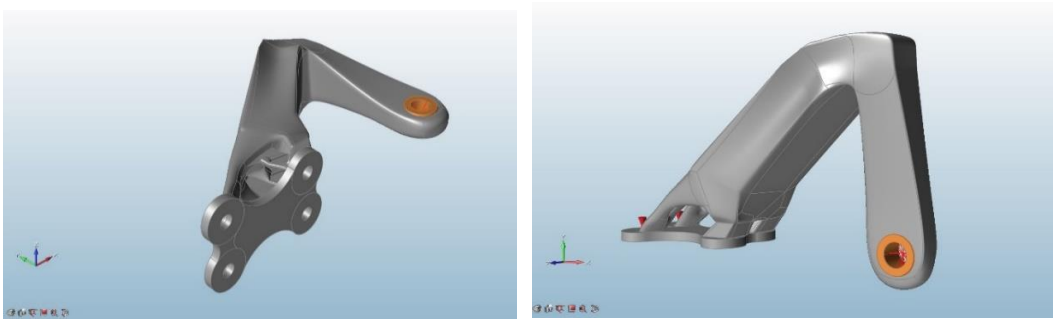

Figure 12: After cleaning the topology optimized result using PolyNURBS feature

As seen from the above figure, the topology optimized result is clean and manufacturable after using the POLYNURBS feature. This solid model can be imported into CAD packages for adding final details and can be manufactured directly. The obtained weight of the final component was reduced by 47%.

Additive manufacturing proves efficient in fabricating organic looking components compared to conventional methods. Figure 13 shows a prototype of this model fabricated using fused deposition modelling process with PLA filament as material.

Figure 13: Pictures of fabricated component

3.3 Hinge Lattice Optimization

Lattice optimization provides a method to create solid components combined with lattice structures which is ideal for additive manufacturing. Lattice optimization is a two-step approach [46] as shown in figure 14.

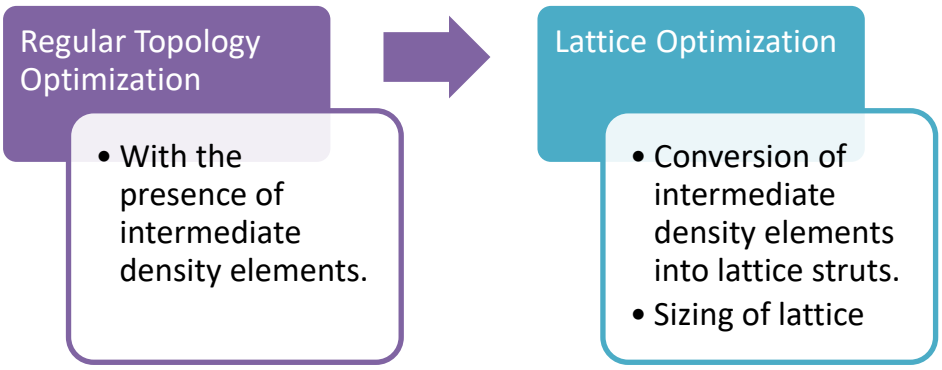

Figure 14: Lattice Optimization Flowchart

In regular topology optimization, the intermediate density elements are treated as fictitious material and are penalized into voids and pure solids. Whereas in lattice optimization, they are converted into lattice structures. During the first phase, regular topology optimization is carried out, except that intermediate density elements are not penalized and are retained within the model [46]. The range of intermediate density elements to be present can be controlled and it will be discussed in the next sub-section. In the second phase, the left out intermediate density elements are converted into lattice structures and the end diameters are sized based on a stress constraint for further fine tuning. In order to perform lattice optimization, LATTICE command should be included in the DTPL bulk data entries as shown in figure 15.

```
.
BEGIN BULK
$$
$$  Stacking Information for Ply-Based Composite Definition
$$

$HMNAME DESVARS        1body
DTPL    1       PSOLID  2
+       DRAW    SPLIT   0.0     0.0     0.0     0.0     0.0     1.0
+       NOHOLE
+       LATTICE 1       0.1     0.8     20000
$$
```

Figure 15: Bulk data section in .fem file

Inclusion of LATTICE command allows the user to specify the cell structure, lower and upper bound for intermediate densities and stress constraint values for lattice sizing. Density values below the lower bound “LB” will be converted into void and values above upper bound “UB” will be converted into solids. Elements between LB and UB are converted into 1D simple beam elements (Type-Rod) and its diameter is proportional to the density of the intermediate density element which were replaced [46]. Figure 16 shows lattice optimized result and the sized lattice end diameters. OptiStruct version 13.0 was

used for lattice optimization and it poses certain limitations such as mesh dependent lattice members and the inability to control the orientation and lattice cell configurations.

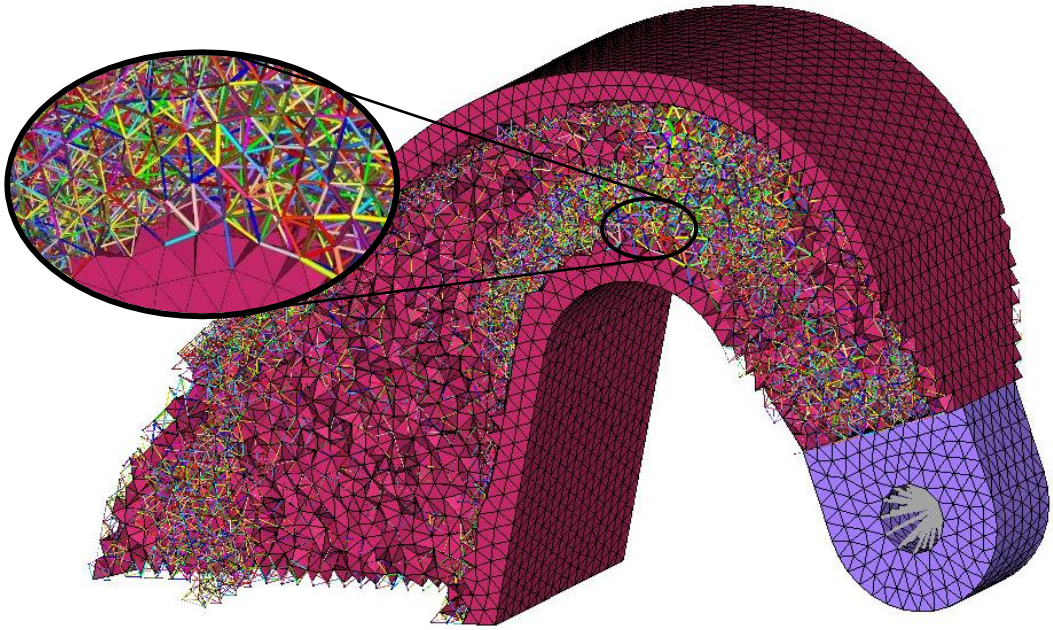

Figure 16: Lattice optimized hinge and sized lattice end diameters

3.3.1 Effect of Range of Intermediate Elements

The use of lattice structures significantly reduces the weight of components but it should be noted that lattice structures display lower stiffness per volume compared to fully dense material which increases the compliance. Hence, the amount of increase in model compliance depends upon the density range of intermediate elements present which are later converted into lattice structures. Stress constraint of 20 ksi is constantly used throughout this work for sizing the lattice diameters in the second phase of optimization. The variation of increase in compliance with varying range of intermediate density elements are shown in figure 17. The open and close loading conditions drive the design in very

similar trends and hence the plot of compliance vs intermediate density element range is explained only for open loading condition.

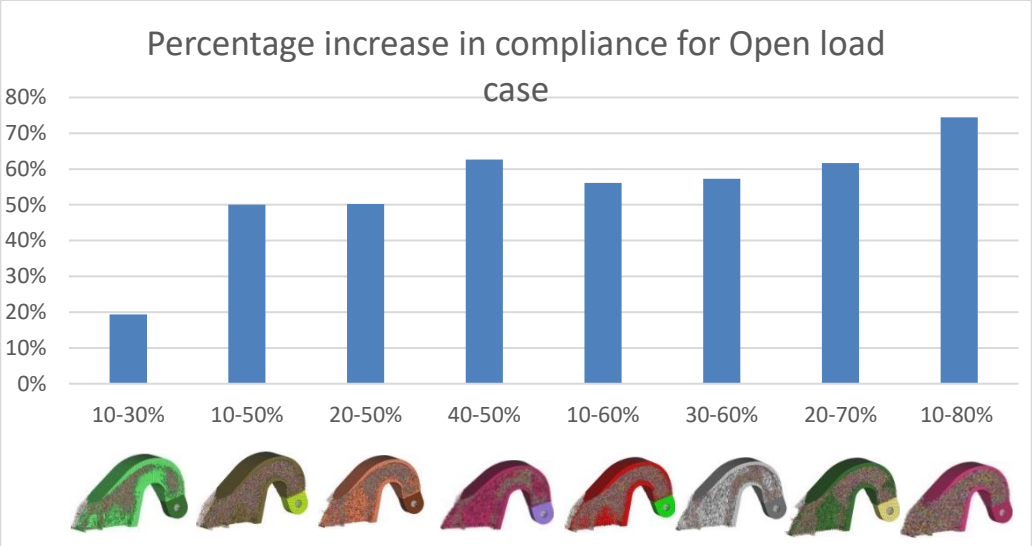

Figure 17: Compliance Vs Intermediate Density Elements Range for Open/Close Loading conditions

It can be seen from the graph that the compliance steadily increases as the upper bound of the intermediate density range increases which means higher the upper bound, larger the number of lattice structures and higher the compliance.

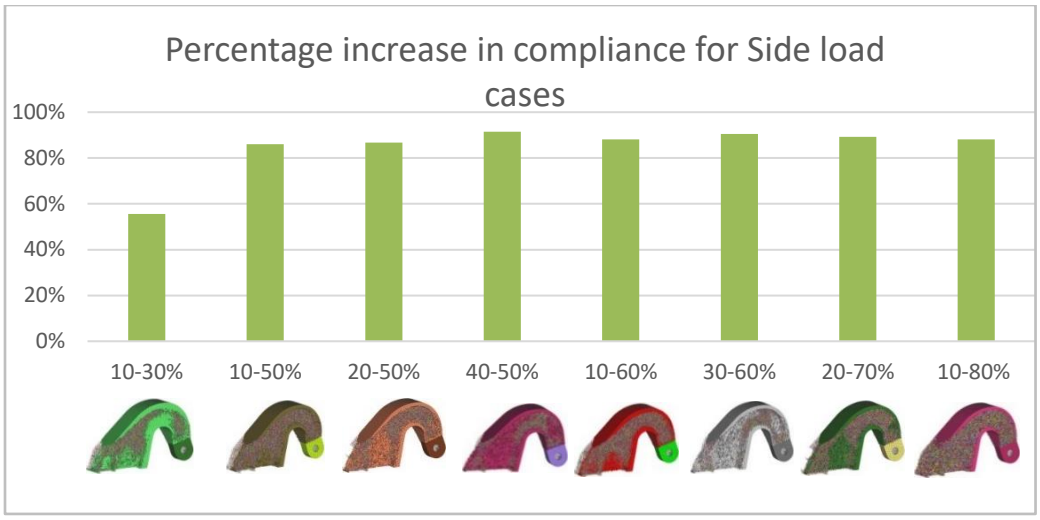

Figure 18: Compliance Vs Intermediate Density Elements

Range for Side Loading condition

The trend which is observed in open/close loading condition cannot be applied to the side loads because side loads puts the hinge under torsion whereas open and close loading conditions causes bending. A box type structure as shown in figure 6 would prove efficient for resisting torsion but as we imposed the draw direction constraint, material along the sides were removed and replaced with lattice structures in lattice optimization due to which the compliance is high for the side loads and remains more or less the same throughout the entire range space variation. During open/close loading, the lattice elements resist shear and during side loads, they resist twisting. Both sets of load cases drives the design differently and it can be observed in plots figure 17 and figure 18.

3.3.2 Effect of Porosity Parameter

From the previous section, it is clearly shown that compliance of the model depends upon the amount of lattice structures present which is controlled by specifying the

range of intermediate density elements. Another way to control the amount of lattice structures present is by using “porosity” parameter [46]. Porosity parameter controls the penalization of intermediate density elements in the first phase of optimization. It is very similar to penalization which occurs during regular topology optimization except that intermediate density elements are retained in the model. Three options are available for this design optimization parameter: High, Medium and Low.

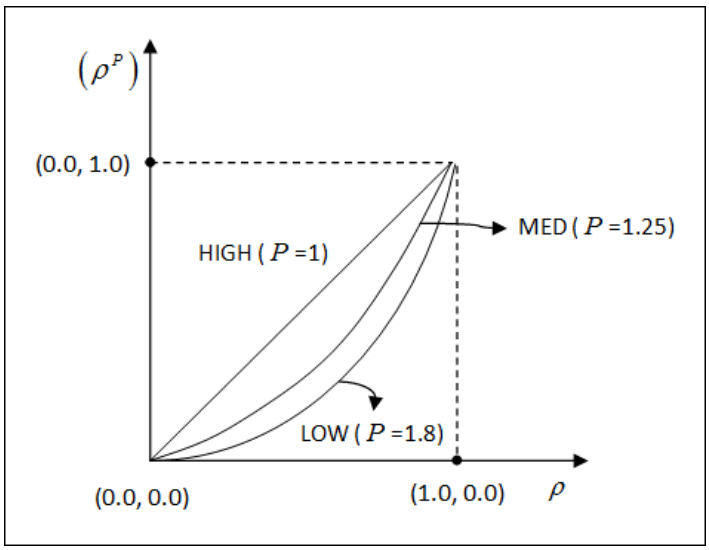

Figure 19: Difference between HIGH, MED and LOW porosity options [47]

From the above graph, if the Porosity value is High, then there is no penalty applied which leads to presence of large amount of intermediate density elements in the first phase which results in high volume fraction [46] of lattice structures in the final design. It is to be noted that the model will have very high compliance due to the large amount of lattice structures. For a Medium porosity value, the penalty applied

is 1.25 which leads to lesser lattice structure zones compared to the previous option. Both High and Medium options are preferred in applications where the component should

be porous. For instance, in the case of a biomedical implants, porosity helps in the growth of tissues over the implants [35]. When the porosity value is Low, a natural penalty of 1.8 is applied which generates very less number of intermediate density elements in the first phase and leads to a design with very low lattice zones and mostly fully dense material distribution. This option is preferred in obtaining a stiffest design (compliance minimization problems). The variation in porosity in shown in figure 20 for lattice optimized model with 10 to 80% intermediate density element range.

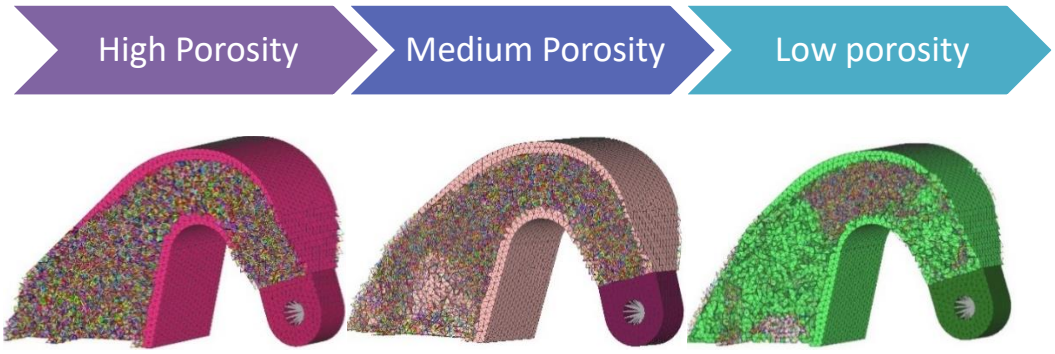

Figure 20: Variation in Porosity parameter: High, Medium and Low

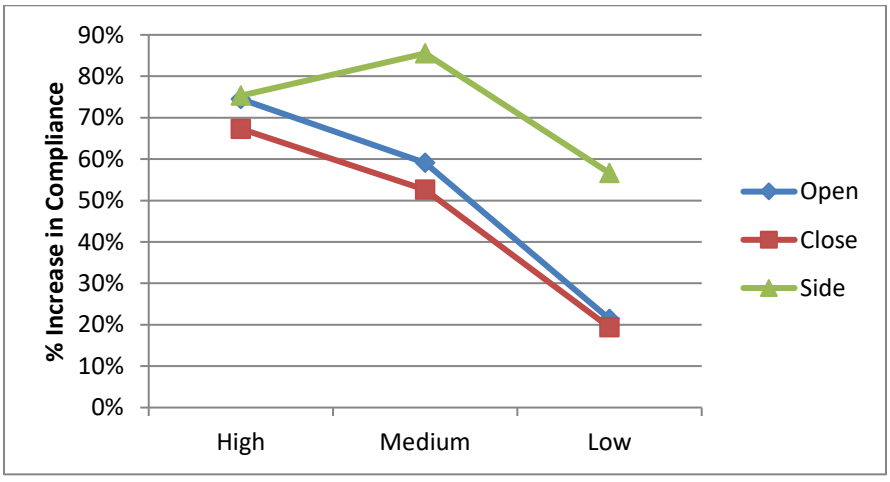

Figure 21: Increase in compliance vs Load cases for various porosity options

Though the above model has a very high intermediate density range of 10 to 80%, it should be noticed that the amount of lattice structures reduces drastically as we move from High to Low and hence there is a decrease in compliance as shown in figure 21. Also, for the low porosity option, the lattice structures are concentrated in the area of stiffeners as predicted by the topology optimized result from figure 7.

Chapter 4

Sizing Optimization and Lattice Structures

Shell model created from the topology optimization result and other model variants with lattice structures along with its sizing optimization results are discussed in this section.

4.1 Hinge Shell Model Details

One might wonder why sizing optimization is required after obtaining topology optimized result. In sizing optimization, the optimum geometrical parameters such as plate thickness for a 2D shell element or diameter for a lattice member is determined. The main feature of sizing optimization is that the structural connectivity of the model is fixed throughout optimization process [48]. Size and shape optimizations are fine tuning optimizations which should be performed after topology optimization because topology optimization provides information only about material distribution in the model, determination of features such as holes and their locations. For instance, for a minimal compliance design, topology optimization adds material along critical load paths and provides the stiffest material distribution in the model. It does not take strength requirements into consideration. Hence, a shell model as shown in figure 22 is developed from the topology optimized result and it is size optimized by taking strength, stability and displacement constraints into account.

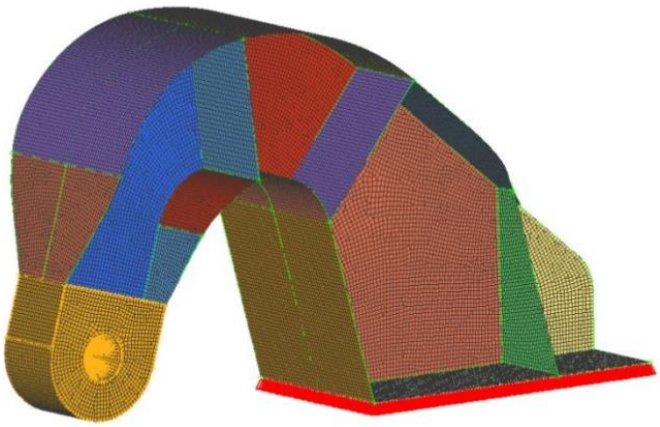

Figure 22: Shell model of the Hinge with Stiffeners

Similar to topology optimization model, the shell model is also constrained by means of six fasteners at its base and has the same loading conditions as shown in figure 5. Gap elements are used at the base of this model as an interface element between two faces of the structure. Gap elements are one-dimensional elements defined by two nodes and are capable of transferring only axial forces (tension and compression) [26]. Here, initially the gap between the base of the hinge and the door is assumed to be closed and there is a load transfer only when the gap elements are in compression (closed condition).

4.2 Hinge Model Variation and Sizing Optimization

In order to understand the relationship between lattice structures and displacement constraint, two other models were created apart from the Shell and Stiffener model (Model-I) as shown in figure 23. Model-II and Model-III consists of lattice structures in place of stiffeners and these lattice structures are imported from lattice optimization result with settings: 10-80% intermediate density range and low porosity option. The main difference between Model-II and Model-III is the diameter of lattice structures. In Model-II, the diameter of lattice structures are the end diameters from the lattice optimized result

whereas in Model-III, the lattice structures are divided into 3 sections along the neck of the hinge: forward, mid and backward region and corresponding sizing variables are created. During the optimization, each section is sized individually so that all the lattice members in a single section has the same diameter.

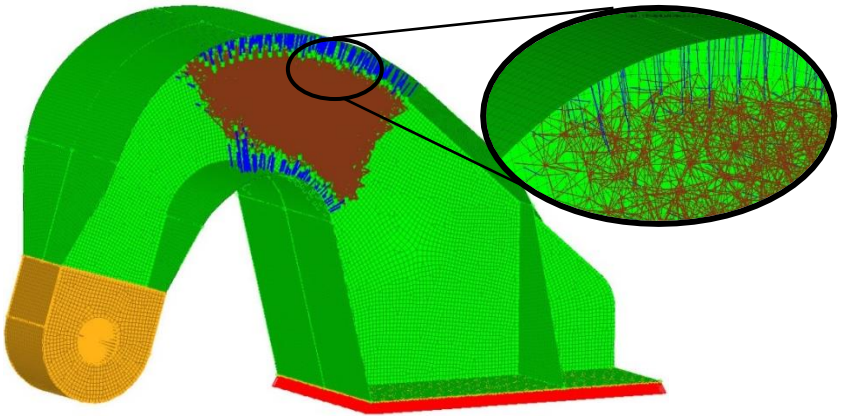

Figure 23: Shell model of the Hinge with Lattice Structures

In order to transmit the load from upper flange to lower flange through lattice structures, the nodes along edges of lattice structure are selected and connected to the flanges by using RBE2 elements. An RBE2 element adds infinite stiffness to the model and transmits displacement from one node to another without any loss.

Similar to topology optimization, OptiStruct uses DRCO approach for sizing optimization as well. The plate thickness of 2D shell elements and diameters of 1D lattice members are the design variables and stress, displacement and mass responses are created. Stress constraints of max/min principal stress: ±40 ksi and displacement constraint of 0.03in are applied for all the 3 model variations. For Model-III, tension and compression stresses of 40 ksi and 20 ksi are given as constraints for sizing the lattice

members. Finally, minimizing the mass is the objective function for this problem and sizing optimization is performed.

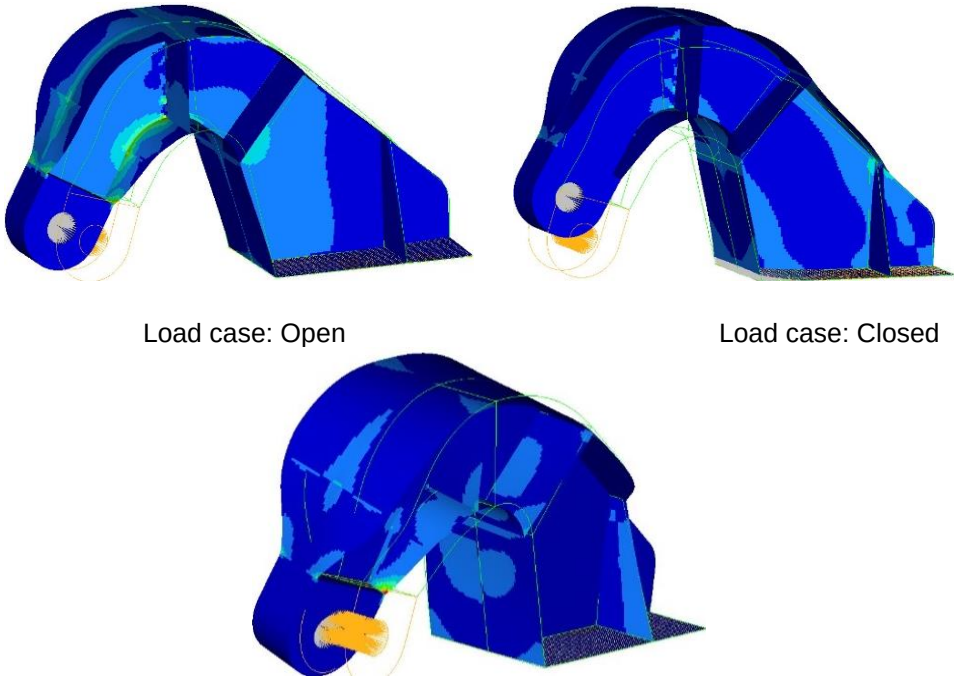

Load case: Open Load case: Closed

Load case: Side

Figure 24: Model-I Von Mises stress plot with deformation for Open, Closed and Side load cases

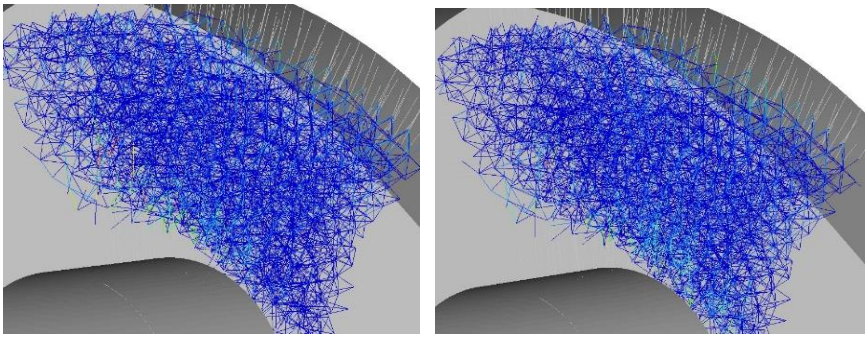

Load case: Open Load case: Closed

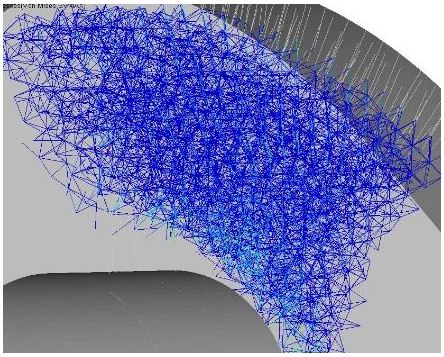

Load case: Side

Figure 25: Model-II Von Mises stress plot for topology sized lattice members for Open, Closed and Side load cases

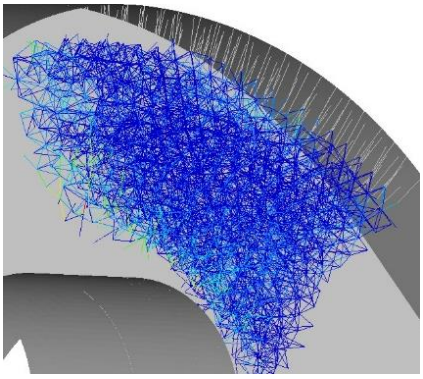

Load case: Open

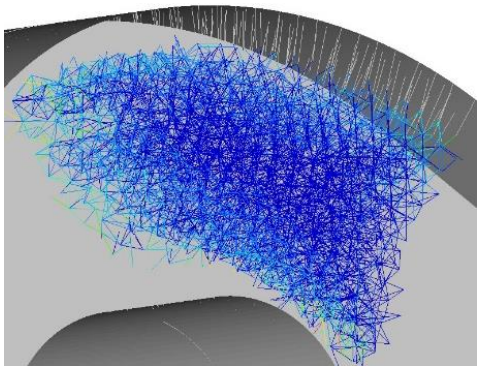

Load case: Closed

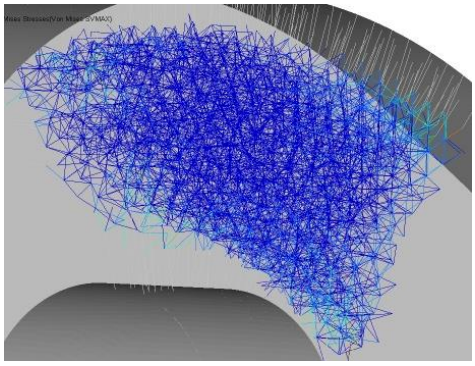

Load case: Side

Figure 26: Model-III Von Mises stress plot for three zone sized lattice members for Open, Closed and Side load cases

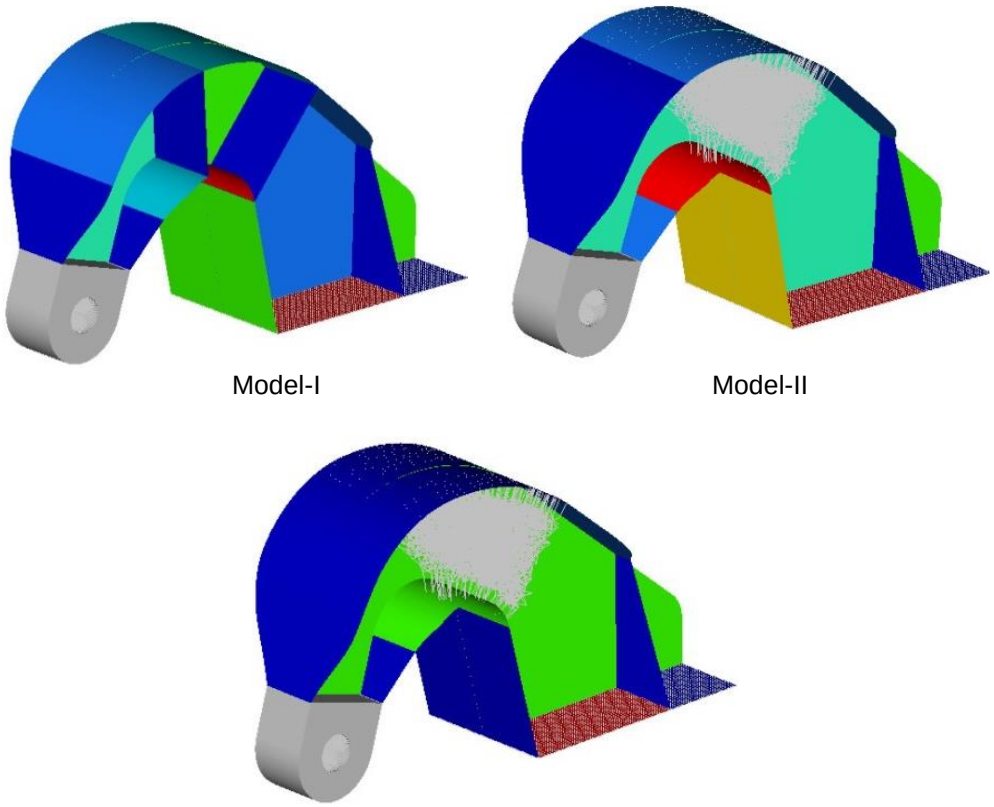

Model-I Model-II

Model-III

Figure 27: Thickness plot for Model-I, Model-II and Model-III

The Von Mises stress plot for all the three models are shown above. From the lattice stress plots, a couple of lattice members reach peak stress especially along the edges where they are tied to the shell flanges using RBE2 elements.

4.3 Mass Comparison for Various Displacement Constraints

As mentioned earlier, though the use of lattice structures reduces the mass of component significantly, it also increases its compliance. In order to benefit from the usage of lattice structures, it is necessary to understand the trend variation between mass and displacement constraint of the component. For this purpose, all the 3 models are size optimized for increasing displacement constraint values and their mass values were recorded. As buckling is an important structural failure mode, the models were optimized by including buckling constraint along with displacement constraint.

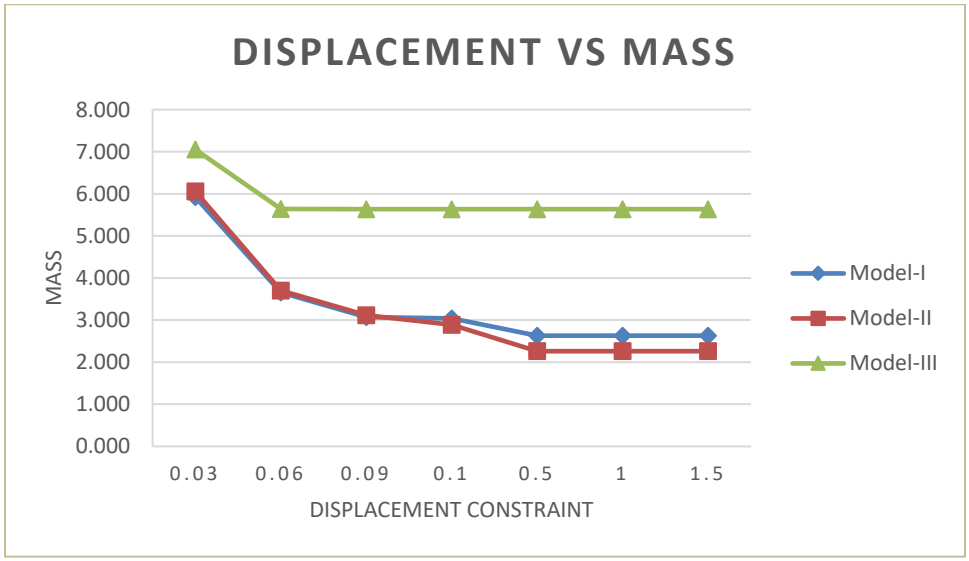

Figure 28: Displacement vs Mass for three model variations

Displacement	Model-I	Model-II	Model-III	%Lattice benefit
0.03	5.92	6.06	7.05	-2%
0.06	3.66	3.70	5.64	-1%
0.09	3.07	3.12	5.64	-2%
0.1	3.04	2.89	5.64	5%
0.5	2.63	2.26	5.64	14%
1	2.63	2.26	5.64	14%
1.5	2.63	2.26	5.64	14%

Table 1: Mass and %Lattice benefit for various Displacement constraints

Table 1 provides information about mass for all the three model variations for increasing displacement values. Here, %lattice benefit denotes the percentage reduction of mass by comparing Model-I and Model-II. The initial negative values are due to noises and various other assumptions in the model. Although mass of Model-I and Model-II are almost the same initially, around 14% of mass reduction can be observed between model with stiffener (Model-I) and model with lattice structures in place of stiffeners (Model-II) once the displacement constraint is relaxed. From figure 28, the variation in trend between displacement and mass is similar in all three design variations as expected i.e. mass of the component reduces if the displacement constraint is relaxed. The displacement-mass curve for Model I and II flattens after 0.5in of displacement because thickness of the shell elements reaches a lower bound value of 0.05in during sizing optimization. From figure 28, it can be seen that Model-III is comparatively heavier than the other models. Due to large number of lattice members, it is difficult to manually hand pick each lattice and create individual design variables. For this purpose, they were segregated into three sections and

sized section wise. As the lattices are sized section wise based on stress, one or two lattice members determine the size of whole section which reduces the design freedom and leads to heavier weight.

Chapter 5

Conclusion and Future Work

This paper can be divided into two sections. In both the sections, a goose neck door hinge with four load cases is used for demonstrating the effects of lattice optimization. In the first half, topology optimization of the model provides an I beam configuration which resists bending during open and close loading conditions and the location of stiffeners. Later, topology optimization is extended to lattice optimization and it should be noted that lattice structures are formed primarily in the place of stiffeners. Compliance of the model depends on the amount of lattice members present which can be controlled using two parameters: range of intermediate density elements and porosity parameter. Figure 17 provides the relationship between range of intermediate density elements and model compliance. It should be observed that the range of intermediate density elements and model compliance are linearly related i.e., model compliance increases as the density range increases. Similarly, porosity parameter can be used to control the amount of lattice structures present which in turn determines the compliance of the model. There are three porosity options: High, Medium and Low. From figure 17 and figure 21, we can come to a conclusion that compliance of the model depends upon the lattice volume fraction i.e., higher the number of lattice members, higher the compliance.

The second half of the paper involves fine tuning of the design. To understand the relationship between lattice structures and displacement constraint, three shell model variations with stiffeners and lattice structures are created where the lattice members are imported from low porosity lattice optimization result. These models are size optimized for increasing displacement constraint values and their corresponding mass values are

recorded. From figure 28 and table 1, it can be noticed that mass of the component reduces as we increase the displacement constraint value and this trend is similar in all three model variations. About 14% mass reduction can be observed between model with stiffener and model with lattice structures once we increase the displacement value. Based on the above observations, lattice structures can be implemented in solid models where low weight is preferred and at the same time relaxation in displacement constraint is acceptable.

HyperMesh and OptiStruct version 13.0 was used for simulation purposes in this paper. The next version 14.0 has been released and research work needs to be done to investigate the changes in results by using the enhancements of latest version. Some of the updated features in lattice optimization are: use of tapered lattice members and lattice smoothing and re-meshing features. Also, lattice structures can be implemented in other applications where it can be used to reduce the component weight without affecting its stiffness. Ways to control the directionality, density, cell configuration and to address the stress concentrations in the lattice structures which might lead to failure will be done in the future work.

Appendix A

FEM Code for Lattice Optimization

A sample FEM code used for setting up optimization parameters to perform lattice optimization is as follows:

```
$$
$$ Optistruct Input Deck Generated by HyperMesh Version  : 11.0.0.47
$$ Generated using HyperMesh-Optistruct Template Version : 11.0.0.47
$$
$$   Template:  optistruct
$$
$$
$$ optistruct
$
SCREEN OUT
$$--------------------------------------------------------------------------$
$$                    Case Control Cards                                    $
$$--------------------------------------------------------------------------$
$$
$$  OBJECTIVES Data
$$
$
$HMNAME OBJECTIVES       1objective
$
DESOBJ(MIN)=2
$
$
DESGLB       2
$
$
$HMNAME LOADSTEP             1"open"       0
$
SUBCASE       1
  SPC =       5
  LOAD =       1
  WEIGHT = 1.0
$
$HMNAME LOADSTEP             2"closed"       0
$
SUBCASE       2
  SPC =       5
  LOAD =       2
  WEIGHT = 1.0
$
$HMNAME LOADSTEP             3"side1"       0
```

Optimization objective definition

Model load case definition

```
$
SUBCASE       3
  SPC =       5
  LOAD =       3
  WEIGHT = 1.0
$
$HMNAME LOADSTEP              4"side2"       0
$
SUBCASE       4
  SPC =       5
  LOAD =       4
  WEIGHT = 1.0
$$---------------------------------------------------------------
$$ HYPERMESH TAGS
$$---------------------------------------------------------------
$$BEGIN TAGS
$$END TAGS
$
BEGIN BULK
$$
$$  Stacking Information for Ply-Based Composite Definition
$$

$HMNAME DESVARS       1body
DTPL    1      PSOLID  2
+       DRAW    SPLIT   0.0     0.0     0.0     0.0     0.0     1.0
+       NOHOLE
+       LATTICE 1       0.1     0.8     20000
$$
$$  OPTIRESPONSES Data
$$
DRESP1  1       volfrac VOLFRAC PSOLID                          2
DRESP1  2       wcomp   WCOMP
$$
$$  OPTICONSTRAINTS Data
$$
$
$HMNAME OPTICONSTRAINTS       1volfrac
$
DCONSTR       1       1       0.4

DCONADD       2       1


$$
```

Model load case definition

Optimization parameters definition

```
$$  DESVARG Data
$$
$$
$$  GRID Data
$$
GRID      74042       5.999988.9999976-.799998
GRID      74043       5.9999880.999998-.533332
.
.
.
.
CTETRA    436220      3   80090   74302   74327   74303
CTETRA    436219      3   80090   80169   80167   74301
CTETRA    436218      3   74371   74394   74368   80089
.
.
.
.
RBE3      563789          98719  1234561.0        123   74065   74055
+         74077   74057   74087   74098   74091   74059   74094   74114
+         74056   74122   74092   74093   74060   74099   74053   74125
.
.
.
.
$$  FORCE Data
$$
FORCE         1   98719      01.0    2000.0  0.0     0.0
FORCE         2   98719      01.0    0.0     2000.0  0.0
FORCE         3   98719      01.0    0.0     0.0     200.0
FORCE         4   98719      01.0    0.0     0.0     -200.0
ENDDATA
```

Grid and element data

Force applied

References

[1] I. Gibson, D. W. Rosen, and B. Stucker, *Additive Manufacturing Technologies*, Second Edi. Springer, 2010.

[2] D. Brackett, I. Ashcroft, and R. Hague, “Topology optimization for additive manufacturing,” *Solid Free. Fabr. Symp.*, pp. 348–362, 2011.

[3] W. Dias and D. Anand, “Design and Optimization of Lattice Structure for 3D Printing using Altair OptiStruct,” 2015. [Online]. Available: http://insider.altairhyperworks.com/design-and-optimization-of-lattice-structures-for-3d-printing-using-altair-optistruct/. [Accessed: 23-May-2016].

[4] M. McMillan, M. Jurg, M. Leary, and M. Brandt, “Programmatic Lattice Generation for Additive Manufacture,” *Procedia Technol.*, vol. 20, no. July, pp. 178–184, 2015.

[5] Y. Tang and Y. F. Zhao, “Lattice-skin Structures Design with Orientation Optimization,” *Proc. Solid Free. Fabr. Symp.*, pp. 1378–1393, 2015.

[6] J. N. Stuecker, J. C. Iii, and E. Smay, “Robocasting Periodic Lattices For Advanced Filtration,” *Solid Free. Fabr. Symp.*, pp. 561–566, 2001.

[7] J. R. Heidrich, V. Gervasi, and S. Kumpaty, “Synthesis of a Compact Tetralattice Heat Exchanger Using Solid Freeform Fabrication and Comparison Testing Against a Tube Heat Exchanger,” *Solid Free. Fabr. Symp.*, pp. 567–575, 2001.

[8] A. Hussein, L. Hao, C. Yan, R. Everson, and P. Young, “Advanced lattice support structures for metal additive manufacturing,” *J. Mater. Process. Technol.*, vol. 213, no. 7, pp. 1019–1026, 2013.

[9] O. Iyibilgin, C. Yigit, and M. C. Leu, “Experimental investigation of different cellular lattice structures manufactured by fused deposition modeling,” *Solid Free. Fabr. Symp.*, pp. 895–907, 2013.

[10] I. Maskery, A. O. Aremu, M. Simonelli, C. Tuck, R. D. Wildman, I. A. Ashcroft, and R. J. M. Hague, “The BCC unit cell for latticed SLM parts ; mechanical properties as a function of cell size .,” *Solid Free. Fabr. Symp.*, pp. 688–701, 2014.

[11] V. S. Deshpande, N. A. Fleck, and M. F. Ashby, “Effective properties of the octet-truss lattice material,” *J. Mech. Phys. Solids*, vol. 49, no. 8, pp. 1747–1769, 2001.

[12] M. Doyoyo and J. W. Hu, “Multi-axial failure of metallic strut-lattice materials composed of short and slender struts,” *Int. J. Solids Struct.*, vol. 43, no. 20, pp. 6115–6139, 2006.

[13] G. N. Labeas and M. M. Sunaric, “Investigation on the Static Response and Failure Process of Metallic Open Lattice Cellular Structures,” *Strain*, vol. 46, no. 2, pp. 195–204, Apr. 2010.

[14] Y. Shen, S. Mckown, S. Tsopanos, C. J. Sutcliffe, R. A. W. Mines, and W. J. Cantwell, “The Mechanical Properties of Sandwich Structures Based on Metal Lattice Architectures,” *J. Sandw. Struct. Mater.*, vol. 12, no. 2, pp. 159–180, Mar. 2010.

[15] E. Masoumi Khalil Abad, S. Arabnejad Khanoki, and D. Pasini, “Fatigue design of lattice materials via computational mechanics: Application to lattices with smooth transitions in cell geometry,” *Int. J. Fatigue*, vol. 47, pp. 126–136, 2013.

[16] “Topology Optimization,” *Wikipedia*, 20-May-2016. [Online]. Available: https://en.wikipedia.org/wiki/Topology_optimization. [Accessed: 01-Jun-2016].

[17] R. T. Haftka and Z. Gürdal, *Elements of structural optimization*. Kluwer Academic Publishers, 1992.

[18] M. P. Bendsøe and N. Kikuchi, “Generating optimal topologies in structural design using a homogenization method,” *Comput. Methods Appl. Mech. Eng.*, vol. 71, no. 2, pp. 197–224, 1988.

[19] G. I. N. Rozvany, “A critical review of established methods of structural topology optimization,” *Struct. Multidiscip. Optim.*, vol. 37, no. 3, pp. 217–237, 2009.

[20] K. Suzuki and N. Kikuchi, “A homogenization method for shape and topology optimization,” *Comput. Methods Appl. Mech. Eng.*, vol. 93, no. 3, pp. 291–318, 1991.

[21] Y. M. Xie and G. P. Steven, “Basic Evolutionary Structural Optimization,” in *Evolutionary Structural Optimization*, London: Springer London, 1997, pp. 12–29.

[22] Y. M. Xie and G. P. Steven, “Evolutionary structural optimization for dynamic problems,” *Comput. Struct.*, vol. 58, no. 6, pp. 1067–1073, 1996.

[23] M. Y. Wang, X. Wang, and D. Guo, “A level set method for structural topology optimization,” *Comput. Methods Appl. Mech. Eng.*, vol. 192, no. 1, pp. 227–246, 2003.

[24] O. Sigmund, “A 99 line topology optimization code written in Matlab,” *Struct. Multidiscip. Optim.*, vol. 21, no. 2, pp. 120–127, Apr. 2001.

[25] E. Andreassen, A. Clausen, M. Schevenels, B. S. Lazarov, O. Sigmund, E. Andreassen, A. Clausen, O. Sigmund, B. Lazarov, and M. Schevenels, “Efficient

topology optimization in MATLAB using 88 lines of code."

[26] "OptiStruct User Guide 14.0," *Altair Connect*, 2016. [Online]. Available: https://connect.altair.com/CP/kb-view.html?f=2&kb=128167. [Accessed: 08-Jun-2016].

[27] "Design variables for topology optimization," *Altair Hyperworks*. [Online]. Available: https://connect.altair.com/CP/kb-view.html?kb=128250. [Accessed: 08-Jun-2016].

[28] J. Nguyen, S. Park, D. W. Rosen, L. Folgar, and J. Williams, "Conformal Lattice Structure Design and Fabrication," *Sff*, pp. 138–161, 2012.

[29] H. V. Wang, Y. Chen, and D. W. Rosen, "A Hybrid Geometric Modeling Method for Large Scale Conformal Cellular Structures," *ASME Comput. Inf. Eng. Conf.*, vol. 2005, pp. 421–427, 2005.

[30] P. S. Chang and D. W. Rosen, "The size matching and scaling method: A synthesis method for the design of mesoscale cellular structures," *Int. J. Comput. Integr. Manuf.*, 2013.

[31] L. Hao, D. Raymont, C. Yan, A. Hussein, and P. Young, "Design and additive manufacturing of cellular lattice structures," *Int. Conf. Adv. Res. Virtual Rapid Prototyp.*, no. May 2016, pp. 249–254, 2012.

[32] S. Park, D. W. Rosen, and C. E. Duty, "Comparing Mechanical and Geometrical Properties of Lattice Structure Fabricated using Electron Beam Melting," *Solid Free. Fabr. Symp.*, pp. 1359–1370, 2014.

[33] J. Chu, S. Engelbrecht, G. Graf, and D. W. Rosen, "A comparison of synthesis methods for cellular structures with application to additive manufacturing," *Rapid Prototyp. J.*, vol. 16, no. 4, pp. 275–283, 2010.

[34] "Altair OptiStruct," *Altair HyperWorks*, 2016. [Online]. Available: http://www.altairhyperworks.com/product/OptiStruct. [Accessed: 30-May-2016].

[35] D. Rosen, S. Johnston, and M. Reed, "Design of General Lattice Structures for Lightweight and Compliance Applications," *Rapid Manuf. Conf.*, pp. 1–14, 2006.

[36] A. Cerardi, M. Caneri, R. Meneghello, and G. Concheri, "Mechanical characterization of polyamide porous specimens for the evaluation of emptying strategies in Rapid Prototyping," in *37th, International matador conference; 2012; Manchester*, 2012.

[37] N. Sudarmadji, J. Y. Tan, K. F. Leong, C. K. Chua, and Y. T. Loh, "Investigation of

the mechanical properties and porosity relationships in selective laser-sintered polyhedral for functionally graded scaffolds," *Acta Biomater.*, vol. 7, no. 2, pp. 530–537, 2011.

[38] E. B. G. Lefevre, "Gooseneck concealed hinge," US2132266 A, 1938.

[39] R. Taylor, D. Durocher, and R. Yancey, "Teaching Aerospace Design Optimization," in *2015 Americas Altair Technology Conference*, 2015, pp. 10–13.

[40] R. Taylor and Y. Martinez, "Leveraging Geometric Shape Complexity in Optimal Design for Additive Manufacturing," in *2015 Americas Altair Technology Conference*, 2015.

[41] "Draw Direction Constraints for Topology Optimization," *Altair HyperWorks*, 2016. [Online]. Available: https://connect.altair.com/CP/kb-view.html?kb=128263. [Accessed: 08-Jun-2016].

[42] "GrabCAD-Airplane Bearing Bracket Challenge," 2016. [Online]. Available: https://grabcad.com/challenges/airplane-bearing-bracket-challenge. [Accessed: 25-Aug-2016].

[43] "Inspire 2016 - PolyNURBS," 2016. [Online]. Available: http://www.engineering.com/DesignSoftware/DesignSoftwareArticles/ArticleID/11700/Inspire-2016-Adds-Organic-PolyNURBS-Finishing-and-Handles-New-Load-Types.aspx. [Accessed: 01-Sep-2016].

[44] "solidThinking Inspire 2016." [Online]. Available: http://www.solidthinking.com/inspire2016.html. [Accessed: 07-Jun-2016].

[45] M. E. Mortenson, *Geometric modeling*. Wiley, 1997.

[46] "Lattice Structure Optimization," *Altair HyperWorks*, 2016. [Online]. Available: https://connect.altair.com/CP/kb-view.html?kb=128259. [Accessed: 13-Jun-2016].

[47] "Lattice Structure Optimization - User Manual," *Altair Connect*. [Online]. Available: https://connect.altair.com/CP/kb-view.html?kb=155005. [Accessed: 01-Nov-2016].

[48] M. P. Bendsøe and O. Sigmund, *Topology optimization: theory, methods, and applications*, vol. 2nd Editio, no. 724. 2003.

Biographical Information

Vignesh Dakshnamoorthy received his Bachelor of Engineering (BE) Degree in Mechanical Engineering from Anna University, Chennai, Tamil Nadu, India. He joined the Department of Mechanical and Aerospace Engineering at the University of Texas at Arlington in August 2014 as a graduate student and earned his Master of Science in Mechanical Engineering in December 2016.